

Research on upconversion luminescence in new $\text{Er}^{3+}/\text{Yb}^{3+}$ codoped oxyfluoride borosilicate glass ceramics

Shilong Zhao (赵士龙), Fei Zheng (郑 飞), Shiqing Xu (徐时清)*,
Huanping Wang (王焕平), and Baoling Wang (王宝玲)

College of Materials Science and Engineering, China Jiliang University, Hangzhou 310018, China

*E-mail: sxucjlu@hotmail.com

Received August 22, 2008

The upconversion luminescence of $\text{Er}^{3+}/\text{Yb}^{3+}$ ions is researched in a novel transparent oxyfluoride borosilicate glass and glass ceramics under 980-nm excitation. Fluoride nanocrystals Ba_2YF_7 are successfully precipitated in glass matrix, which is affirmed by the X-ray diffraction results. Compared with the parent glasses, significant enhancement of upconversion luminescence is observed in the $\text{Er}^{3+}/\text{Yb}^{3+}$ codoped transparent glass-ceramics, which may be due to the variation of coordination environment around Er^{3+} and Yb^{3+} ions after crystallization. The possible upconversion mechanism is also discussed.

OCIS codes: 160.4760, 160.5690.

doi: 10.3788/COL20090705.0416.

Oxyfluoride glasses and glass ceramics are one of the most attractive hosts for rare earth doping, which not only provide a low phonon energy environment for active rare-earth ions but also possess good mechanical and chemical stability in a material^[1-4]. Auzel *et al.* firstly reported an oxyfluoride glass ceramic^[5], and Wang *et al.* successfully fabricated $\text{Er}^{3+}/\text{Yb}^{3+}$ codoped transparent oxyfluoride glass ceramics^[6]. These glass ceramics exhibited efficient infrared (IR) to visible upconversion under 980-nm excitation. In order to develop highly efficient upconversion glass ceramics, the key factor is to search for the appropriate fluoride nano-crystalline host for rare-earth ions^[7]. Ba_2YF_7 was firstly prepared by Rao *et al.*^[8] and its structural analogy Ba_2YCl_7 doped with erbium ions exhibited highly efficient upconversion luminescence^[9], so it was expected that Er^{3+} -doped Ba_2YF_7 may be a favorable upconversion material. Furthermore, there are few reports on the upconversion luminescence of rare earth ions in oxyfluoride borosilicate glasses ceramics^[10]. In this letter, an $\text{Er}^{3+}/\text{Yb}^{3+}$ codoped oxyfluoride borosilicate glass ceramics containing Ba_2YF_7 nanocrystals is successfully prepared and its upconversion luminescence is investigated.

The parent glass was prepared with the composition in molar ratio of $55\text{SiO}_2-15\text{B}_2\text{O}_3-18\text{Na}_2\text{O}-10\text{BaF}_2-5.5\text{YF}_3-0.1\text{ErF}_3-0.4\text{YbF}_3$. The mixed materials were melted in an alumina crucible at 1350 °C for about 40 min. Then the glass was quenched into a preheated brass mold. The quenched sample was annealed at 450 °C for 2h and cooled slowly to release the thermal stress associated with these glasses during the quenching process. The differential thermal analysis (DTA) result of the oxyfluoride borosilicate glass shows that the transition temperature is 490 °C, and a weak crystallization peak occurs at 690 °C. Therefore, crystallization conditions of 560, 580, 600, and 620 °C for 2 h were selected to form transparent glass ceramics, and the samples were named as GC560, GC580, GC600, and GC620, respectively.

X-ray diffraction (XRD) measurements were performed in an X'TRA diffractometer with $\text{Cu-K}\alpha$ radiation

at 4-deg./min scanning rate. Transmittance spectra were obtained with an ultraviolet/visible/near-infrared (UV/VIS/NIR) 3150 spectrophotometer. Upconversion luminescence spectra of Er^{3+} ions were measured with a Jobin-Yvon Frolog 3 fluorescence spectrophotometer under the excitation of a 980-nm laser diode (LD). All measurements were taken at room temperature.

The XRD patterns of $\text{Er}^{3+}/\text{Yb}^{3+}$ codoped parent glass and glass ceramics are shown in Fig. 1. The parent glass is completely amorphous with no obvious diffraction peaks. After heat treatment, XRD patterns show intense diffraction peaks, which are easily assigned to the Ba_2YF_7 crystal^[8]. With the increase of heat treatment temperature, the diffraction peaks become sharper, which indicates the increase of crystalline phase. From the peak width of XRD pattern, the crystal size of Ba_2YF_7 crystals in the glass matrix can be estimated by using Scherrer's equation: $D = K\lambda/\beta\cos\theta$, where D is the crystal size at the vertical direction of (hkl) , λ is the wavelength of X-ray, θ is the angle of diffraction, β is the corrected full-width at half-maximum (FWHM) of the diffraction peak, and the constant K is determined by β and the instrument. The calculated mean sizes of the Ba_2YF_7 crystals are about 12, 18, 25, and 35 nm for GC560, GC580, GC600, and GC620, respectively.

Figure 2 displays the transmittance spectra of the

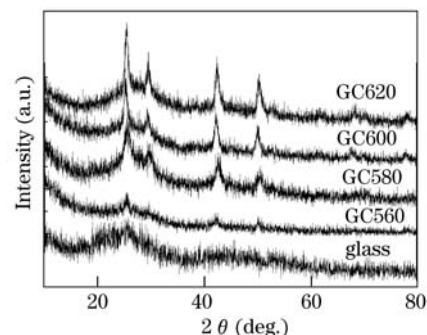


Fig. 1. XRD patterns of the parent glass and glass ceramics.

$\text{Er}^{3+}/\text{Yb}^{3+}$ codoped parent glass and glass ceramics. Compared with the very transparent samples of parent glass and GC-560, the transparency of GC-580 and GC-600 decreases. However, the glass ceramics still remain high transparency, where the transmittance of glass ceramic around 450 nm is above 70%. When the heat treatment temperature reaches 620°C, the transmittance of GC-620 drops rapidly and the sample becomes slightly opaque.

The upconversion luminescence spectra of Er^{3+} ions sensitized by Yb^{3+} ions under 980-nm LD excitation (200-mW) in the parent glass and glass ceramics are shown in Fig. 3. The emission bands can be assigned to ${}^2H_{11/2} \rightarrow {}^4I_{15/2}$ (520 nm), ${}^4S_{3/2} \rightarrow {}^4I_{15/2}$ (540 nm), and ${}^4F_{9/2} \rightarrow {}^4I_{15/2}$ (655 nm) transitions, respectively. Compared with the parent glass, significant enhancement of upconversion luminescence is observed in the $\text{Er}^{3+}/\text{Yb}^{3+}$ codoped transparent glass ceramics. Especially, the upconversion emission intensity at 540 nm increases by a factor of 200 after heat treatment for GC600. It is well known that the intensity of upconversion luminescence is very sensitive to the multiphonon relaxation rate of the rare-earth ions, which strongly depends on the phonon energy of the ion matrix. Usually, the lower the phonon energy of host is, the smaller the multiphonon relaxation probability is. The maximum phonon energy in silicate oxide glass is about 1100 cm^{-1} and that in borate oxide glass is about 1400 cm^{-1} , respectively. However, the maximum phonon energy of BaF_2 is 346 cm^{-1} [11], and that of YF_3 is 533 cm^{-1} [12], which are significantly lower than those in the parent glasses. Therefore, the maximum phonon

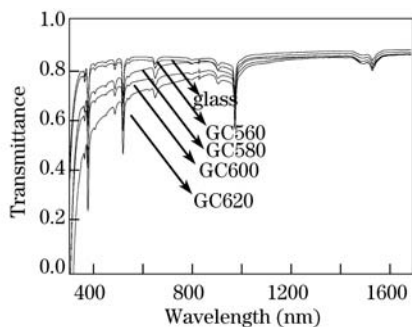


Fig. 2. Transmittance spectra of the $\text{Er}^{3+}/\text{Yb}^{3+}$ codoped parent glass and glass ceramics.

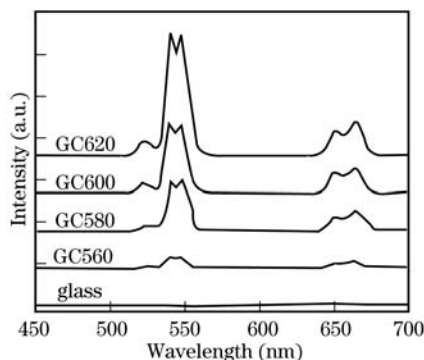


Fig. 3. Upconversion spectra of Er^{3+} ions in the glass and glass ceramics under 980-nm excitation.

energy of Ba_2YF_7 nanocrystals is much lower than that of the parent glass. Thus, the variation of coordination environment around Er^{3+} and Yb^{3+} ions after crystallization may result in the significant enhancement of upconversion luminescence intensity in the glass ceramics.

In the upconversion processes, there is the following relation between the upconversion emission intensity I_{em} and the IR excitation intensity I_{ex} : $I_{\text{em}} \propto (I_{\text{ex}})^n$, where n is the number of IR photons absorbed per visible photon emitted. Therefore, a plot of $\log(I_{\text{em}})$ versus $\log(I_{\text{ex}})$ should yield a straight line with the slope n , as shown in Fig. 4 for the sample GC600. The slopes of 520-, 540-, and 655-nm emissions are 1.97, 1.77, and 1.86, respectively. These results indicate that the green and red emission mechanism can be described as a two-photon mechanism.

The possible upconversion mechanism of $\text{Er}^{3+}/\text{Yb}^{3+}$ ions is proposed, as depicted in Fig. 5. Firstly, the ${}^4I_{11/2}$ level of Er^{3+} ions is directly excited with 980-nm light by means of ground state absorption (GSA) and/or by energy transfer (ET) process from ${}^2F_{5/2}$ level of Yb^{3+} : ${}^2F_{5/2}(\text{Yb}^{3+}) + {}^4I_{15/2}(\text{Er}^{3+}) \rightarrow {}^2F_{7/2}(\text{Yb}^{3+}) + {}^4I_{11/2}(\text{Er}^{3+})$. Since both Er^{3+} and Yb^{3+} ions are incorporated into the crystalline phase and Yb^{3+} has a much larger absorption cross-section than Er^{3+} in the 980-nm region, the ET process is dominant for the excitation of ${}^4I_{11/2}$ level. Secondly, the excitation processes based on the long-lived ${}^4I_{11/2}$ level occur as follows: excited state absorption (ESA), ${}^4I_{11/2}(\text{Er}^{3+}) + \text{a photon} \rightarrow {}^4F_{7/2}(\text{Er}^{3+})$; ET, ${}^2F_{5/2}(\text{Yb}^{3+}) + {}^4I_{11/2}(\text{Er}^{3+}) \rightarrow {}^2F_{7/2}(\text{Yb}^{3+}) + {}^4F_{7/2}(\text{Er}^{3+})$ and ${}^4I_{11/2}(\text{Er}^{3+}) + {}^4I_{11/2}(\text{Er}^{3+}) \rightarrow {}^4I_{15/2}(\text{Er}^{3+}) + {}^4F_{7/2}(\text{Er}^{3+})$. The populated ${}^4F_{7/2}$ level of Er^{3+} ions then decays non-radiatively to the next lower energy states ${}^2H_{11/2}$ and ${}^4S_{3/2}$, and the latter transmit to the ground state and produce the 520- and 540-nm green emissions, respectively. The red emission at 655 nm is originated from the ${}^4F_{9/2} \rightarrow {}^4I_{15/2}$ transition. There exist two main possible pumping mechanisms for the 655-nm red emission. The first possible mechanism is that the ${}^4S_{3/2}$ state of Er^{3+} ions decays non-radiatively to the lower energy state ${}^4F_{9/2}$ through a multiphonon relaxation process. In another possible mechanism, the population of ${}^4F_{9/2}$ is based on the processes as follows: ET from Yb^{3+} , ${}^2F_{5/2}(\text{Yb}^{3+}) + {}^4I_{13/2}(\text{Er}^{3+}) \rightarrow$

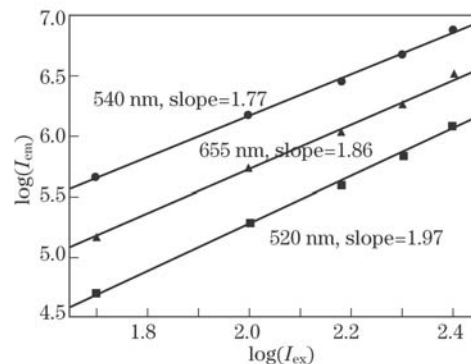


Fig. 4. Log-log plot of upconversion emission intensity (a.u.) as a function of excitation power (mW) for the sample GC600.

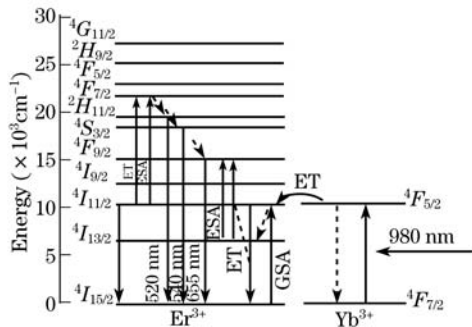


Fig. 5. Simple energy level diagram of Er^{3+} and Yb^{3+} ions and possible upconversion mechanism.

${}^2F_{7/2}(\text{Yb}^{3+}) + {}^4F_{9/2}(\text{Er}^{3+})$; ET between Er^{3+} ions, ${}^4I_{13/2} + {}^4I_{11/2} \rightarrow {}^4I_{15/2} + {}^4F_{9/2}$; ESA, ${}^4I_{13/2} + \text{a photon} \rightarrow {}^4F_{9/2}$. The ${}^4I_{13/2}$ level is populated owing to the non-radiative relaxation from the upper ${}^4I_{11/2}$ level. The populated ${}^4F_{9/2}$ excited state transmits to the ground state and gives the 655-nm red luminescence.

In conclusion, the novel transparent $\text{Er}^{3+}/\text{Yb}^{3+}$ codoped oxyfluoride borosilicate glass ceramics containing Ba_2YF_7 crystals have been prepared. Intense upconversion luminescence of Er^{3+} was observed in the glass ceramics. The transition mechanism of the green and red emissions can be ascribed to a two-photon absorption process. Due to their high transparency and strong upconversion luminescence, the novel $\text{Er}^{3+}/\text{Yb}^{3+}$ codoped oxyfluoride borosilicate glass ceramics may be a promising candidate host matrix for the compact solid-state short-wavelength lasers.

This work was supported by the National Natural Sci-

ence Foundation of China (Nos. 60508014 and 50772102), the Program for New Century Excellent Talents in University (NCET-07-0786), the Science Technology Project of Zhejiang Province (No. 2008C21162), the China Postdoctoral Science Foundation (No. 20080430216), and the Nature Science Foundation of Zhejiang Province (No. R406007).

References

1. F. Liu, E. Ma, D. Chen, Y. Yu, and Y. Wang, *J. Phys. Chem. B* **110**, 20843 (2006).
2. H. Yu, L. Zhao, J. Meng, Q. Liang, X. Yu, B. Tang, and J. Xu, *Chin. Opt. Lett.* **3**, 469 (2005).
3. Y. Zhou, J. Wang, S. Dai, X. Shen, T. Xu, and Q. Nie, *Chinese J. Lasers (in Chinese)* **34**, 1688 (2007).
4. M. Beggiora, I. M. Reaney, and M. S. Islam, *Appl. Phys. Lett.* **83**, 467 (2003).
5. F. Auzel, D. Pecile, and D. Morin, *J. Electrochem. Soc.* **122**, 101 (1975).
6. Y. Wang and J. Ohwaki, *Appl. Phys. Lett.* **63**, 3268 (1993).
7. F. Liu, Y. Wang, D. Chen, Y. Yu, E. Ma, L. Zhou, and P. Huang, *Mater. Lett.* **61**, 5022 (2007).
8. U. R. K. Rao, A. K. Tyagi, K. V. Muralidharan, and R. M. Iyer, *J. Mater. Sci. Lett.* **11**, 435 (1992).
9. P. Egger, P. Rogin, T. Riedener, H. U. Güdel, M. S. Wickleder, and J. Hulliger, *Adv. Mater.* **8**, 668 (1996).
10. M. Środa, *J. Therm. Anal. Calorim.* **88**, 245 (2007).
11. S. A. Pollack and D. B. Chang, *J. Appl. Phys.* **64**, 2885 (1988).
12. W. R. Wilmarth, G. M. Begun, S. E. Nave, and J. R. Peterson, *J. Chem. Phys.* **89**, 711 (1988).